Preprints (www.preprints.org) | NOT PEER-REVIEWED | Posted: 4 October 2017 doi:10.20944/preprints201708.0020.v3

ANALYSIS OF A REGIONAL SCALE CHEMICAL-TRANSPORT MODEL TO INVESTIGATE THE POTENTIONAL CAPABILTY OF SATELLITES FOR IDENTIFYING A WIDESPREAD AIR POLLUTION EVENT

Jason R. Welsh and Jack Fishman
Department of Earth and Atmospheric Sciences
Saint Louis University
St. Louis MO 63108 USA

Abstract

We use a regional scale photochemical transport model to investigate the surface concentrations and column integrated amounts of ozone (O_3) and nitrogen dioxide (NO_2) during a pollution event that occurred in the St. Louis metropolitan region in 2012. These trace gases will be two of the primary constituents that will be measured by TEMPO (Tropospheric Emissions: Monitoring of Pollution), an instrument on a geostationary platform, which will result in a dataset that has hourly temporal resolution during the daytime and ~4 km spatial resolution. Although air quality managers are most concerned with surface concentrations, satellite measurements provide a quantity that reflects a column amount, which may or may not be directly relatable to what is measured at the surface. Our model results provide reasonably good agreement with observed surface O_3 concentrations (correlation coefficients ranging from 0.69 to 0.87 at each of the nine monitoring stations in the St. Louis region), which is the only trace gas dataset that can be used for verification. The model shows that a plume of O_3 extends downwind from St. Louis and contains an integrated amount of ozone of ~ 16 Dobson Units (DU; 1 DU = 2.69×10^{16} molecules cm^{-2}), an amount lower than what was observed during two massive pollution episodes in the 1980s. Based on the smaller isolatable emissions coming from St. Louis, this quantity is not unreasonable, but may also reflect the reduction of photochemical ozone production due to the implementation of emission controls that have gone into effect since the 1980s.

Key Words:
Tropospheric ozone; pollution episode; satellite measurements; regional transport

© 2017 by the author(s). Distributed under a Creative Commons CC BY license.

Preprints (www.preprints.org) | NOT PEER-REVIEWED | Posted: 4 October 2017 doi:10.20944/preprints201708.0020.v3

I. INTRODUCTION

More than three decades have passed since Fishman et al. (1987) showed that photochemically generated ozone air pollution events could be inferred using solar backscattered ultraviolet radiation measurements from satellite sensors. That study identified a synoptic-scale ozone pollution event that evolved over several days and illustrated how enhanced surface ozone observations were embedded within total ozone measurements made by the TOMS (Total Ozone Mapping Spectrometer) instrument. In subsequent studies, Fishman et al. (1990; 2003) provided a methodology that was able to separate tropospheric ozone from the total ozone column using independent concurrent measurements from other instruments such as SAGE (Stratospheric Aerosol Gas Experiment) and SBUV (Solar Backscatter Ultraviolet), which were used to construct stratospheric ozone profiles. These stratospheric ozone profiles were then subtracted from TOMS total ozone amounts to produce a quantity known as tropospheric ozone residual (TOR). Similarly, the use of concurrent total ozone quantities from OMI (Ozone Monitoring Instrument) and stratospheric ozone profiles derived from the MLS (Microwave Limb Scanning) instruments aboard the Aura satellite launched in 2004 have provided an impressive dataset, defined as tropospheric column ozone (TCO; Ziemke et al. 1998; 2006; Levelt et al., 2017). Both the TOR and TCO have provided valuable insight into the global distribution of the amount of ozone in the troposphere, and how these distributions relate to the use of fossil fuel in the northern hemisphere as well as widespread biomass burning in the tropics.

With respect to their use for air pollution studies, measurements from OMI, multiple versions of the GOME (Global Ozone Monitoring Experiment), and the SCIAMACHY (SCanning Imaging Absorption spectroMeter for Atmospheric CHartographY) instruments have provided nitrogen dioxide (NO_2) column measurements that clearly show the distribution of the emissions on scales of only a few kilometers (e.g., Russell et al., 2012; Duncan et al., 2016). Using measurements of high-resolution UV/Vis spectra to which the technique of differential optical absorption spectroscopy (DOAS) is applied (Platt and Stutz, 2008), numerous

Preprints (www.preprints.org) | NOT PEER-REVIEWED | Posted: 4 October 2017 doi:10.20944/preprints201708.0020.v3

studies have shown that well-defined spatial emission patterns of NO_2 within urban areas can be identified. These analyses have been used to identify weekday-vs.-weekend differences in major cities, and, perhaps most significantly, long-term trends in NO_2 emissions, which highlight the impact of regulations imposed on them since the early 2000s (Duncan et al., 2016). Figure 1 (from Lu et al., 2015) shows how the relationships between NO_2 emissions can be inferred from satellite-derived measurements.

Despite the success of using satellite measurements for deriving insight into NO_2, the challenge remains in defining a measureable relationship between what is observed from satellites, which is a column measurement, and what is observed at the surface; which, from an air quality manager's perspective, is the quantity that determines whether or not a region meets National Ambient Air Quality Standards (NAAQS; https://www.epa.gov/criteria-air-pollutants/naaqs-table) criteria and thus, whether or not a specific region is in compliance. This study will focus on the relationship between ozone observed at the surface and how integrated quantities obtained from satellite measurements (which is what satellites observe) relate to each other.

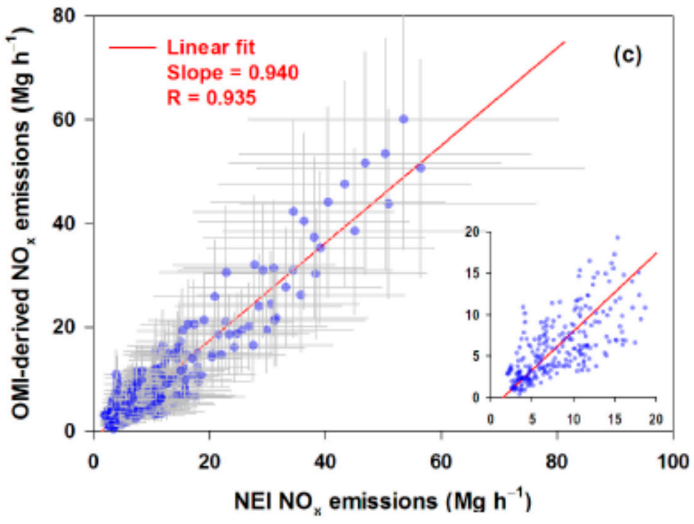

Figure 1. Comparison of satellite-derived and bottoms-up emissions estimates (from Lu et al., 2015)

Preprints (www.preprints.org) | NOT PEER-REVIEWED | Posted: 4 October 2017 doi:10.20944/preprints201708.0020.v3

II Methodology: Model Description and Synoptic Situation

For analytical purposes, we use a model that can simulate the trace gases of interest at the same temporal and spatial resolution that would be observed from space by TEMPO. We used the Comprehensive Air quality Model with eXtensions (CAMx) to calculate the trace gas distributions discussed in this study. CAMx is an Eulerian regional photochemical dispersion model used to examine air pollution over many different scales, ranging from neighborhoods to continents. The meteorological input for the model calculations described below, were taken from simulations from the WRF (Weather Research and Forecasting) model (http://www.wrf-model.org/index.php) which was run with a 4-km resolution over our domain of interest, then embedded in a domain with a 12-km resolution from 34°N to 44°N in the north-south direction and from 86°W to 96°W in the east-west direction; a region that includes all of Missouri, Illinois and Indiana and adjacent areas north and south. The model was run from 20 June through 6 July and of that output, the last five days of those calculations were used as our case study. The most significant day of interest was July 2, 2012, where the highest concentrations of ozone were observed during that summer. Furthermore, 2012 was the most polluted summer of the decade between 2006 and 2016 in St. Louis.

During this study, the temperature and wind fields generated by WRF were consistent with what is often present for that time of year, and weak southwesterly winds prevailed in the St. Louis region. Throughout the extended 10-day period from 28 June through 7 July, temperatures consistently >37.8°C (100°F) were measured daily and record high temperatures were recorded for eight of those ten days in St. Louis. On a larger scale, the Midwest experienced considerably drier than average conditions; nationally, the July average temperature was 25.3°C (77.6 ◦F), the warmest July and warmest month on record dating back to 1895.

Preprints (www.preprints.org) | NOT PEER-REVIEWED | Posted: 4 October 2017 doi:10.20944/preprints201708.0020.v3

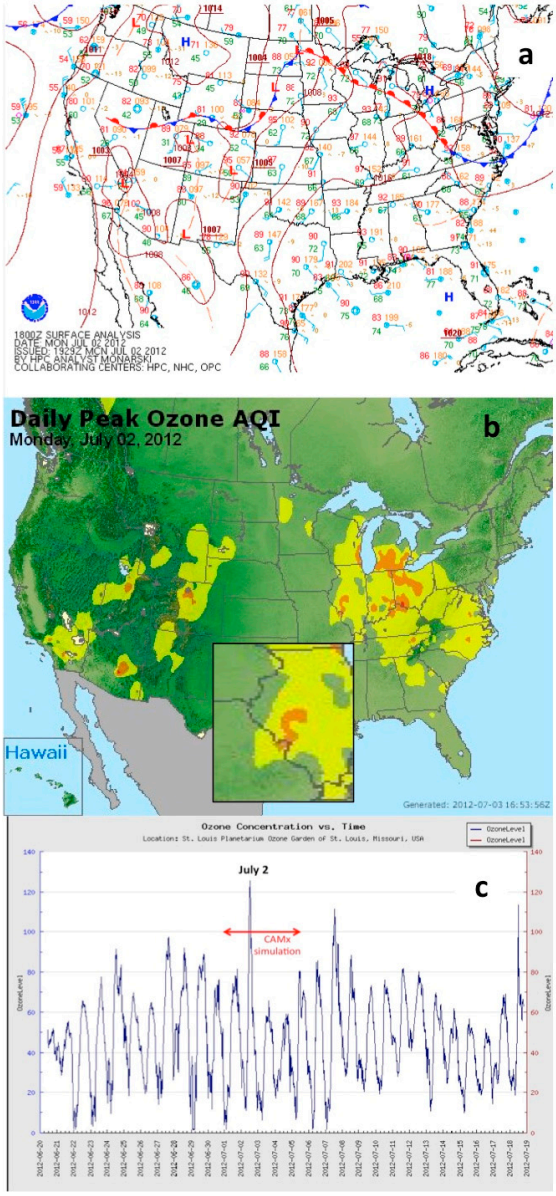

Figure 2 (a). Synoptic weather map showing July 2, 2012 at 1800 UTC (1:00 p.m CDT) surface analysis. (b) AQI Ozone map for July 2, 2012; enlargement of the St. Louis region is inserted in the lower portion of this panel. (c) Ozone concentrations recorded at the St. Louis Planetarium between June 20 and July 7, 2012. Also shown on this plot is the 5-day period when the CAMx model was run for this study. The highest O_3 concentration measured during the entire summer occurred on July 2nd.

Preprints (www.preprints.org) | NOT PEER-REVIEWED | Posted: 4 October 2017 doi:10.20944/preprints201708.0020.v3

The surface map for 2 July at 1800Z (1300 CDT) is shown in Figure 2a. Most of the region in the eastern U.S. is dominated by high pressure with a weak High identified in the Gulf of Mexico off the coast of Florida. A weak frontal system is seen throughout the northern states, resulting in light, generally southwesterly, winds dominating the weather pattern in the St. Louis region. As a result, with this typical summertime Bermuda High dominating much of the North American continent, precipitation formation was also inhibited and many afternoon thunderstorms that are often triggered by afternoon heating from the sun did not develop.

The occurrence of high ozone formation will likely occur when light winds and high temperatures are present with sufficiently high concentrations of NO_x. A map of the EPA Air Quality Index (AQI) for ozone is shown in Figure 2b. Although the eastern U.S. is dominated by a situation conducive to the photochemical generation of high amounts of ozone, most of the region is characterized by only moderately high ozone concentrations. A few pockets in the AQI "orange" range (unhealthy for sensitive groups; 71-85 ppb) are present and a plume of elevated ozone is seen originating over the St. Louis urban area and transported by the prevailing southwesterly winds (insert of Fig. 2b).

From the end of June through much of July, the St. Louis Metropolitan Area experienced high ozone concentrations throughout the region. Figure 2c shows the ozone concentration between 20 June and 7 July 2012. High O_3 concentrations were also measured for much of that period, as shown in Figure 2c. The measurements depicted in this plot are taken from the St. Louis Ozone Garden (Fishman et al., 2014), located in Forest Park, close to the center of the city. The AQS monitoring data has only a 1-hour resolution whereas the monitor at this site records data every 15 minutes. Also shown in this figure is the 5-day time period of the CAMx simulation and the concentration measured on July 2nd, the day when the site measured its highest concentration of the summer at 126 ppb.

Preprints (www.preprints.org) | NOT PEER-REVIEWED | Posted: 4 October 2017 doi:10.20944/preprints201708.0020.v3

III. Results

From an air quality perspective, the most widely available dataset are the surface ozone measurements and we compare our model results with these observations. Overall, there is reasonable agreement between the model-derived results and the observations, as shown in Figure 3 which compares the average concentrations over the entire region with results from the 5-day model run. The solid lines are average concentrations taken from measurements nine stations in the greater St. Louis region. The model calculations (dashed lines) capture the daily maximum concentrations reasonably well (within 5-10 ppb) for each of the days simulated except on 4 July, where the calculated maximum value is 88 ppb, compared an observed concentration of 60 ppb.

Agreement between calculations and observations at night are not as good where model-derived surface concentrations are higher than what is observed. However, since this study is primarily concerned with comparing integrated daytime column amounts (which is when satellite measurements will be made) to surface concentrations, it is most important that the daytime model simulations are in reasonable agreement.

A map of correlation coefficients of all the stations that made measurements during these 5 days and the calculated surface concentrations is shown in Figure 4. These correlation coefficients are based on hourly observations during daylight hours and the calculated coincident hourly values at each station; they range between 0.69 and 0.87.

Preprints (www.preprints.org) | NOT PEER-REVIEWED | Posted: 4 October 2017 doi:10.20944/preprints201708.0020.v3

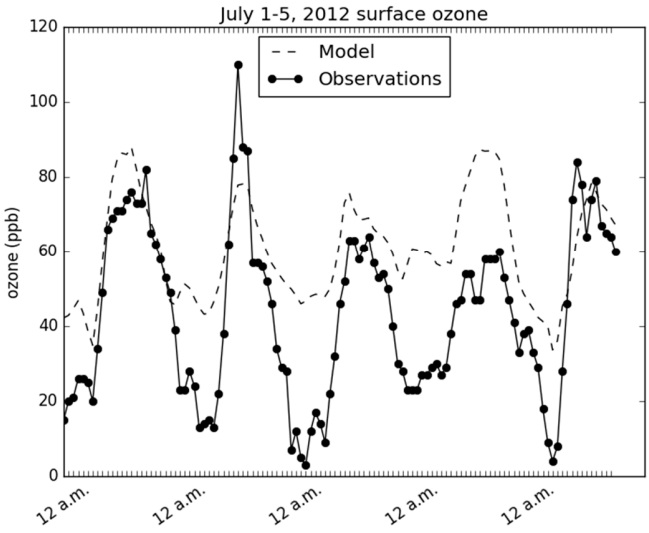

Figure 3. Solid line depicts the average O_3 concentrations from the St. Louis AQS stations compared with the model-derived O_3 concentrations (dashed line) during the period July 1-5, 2012

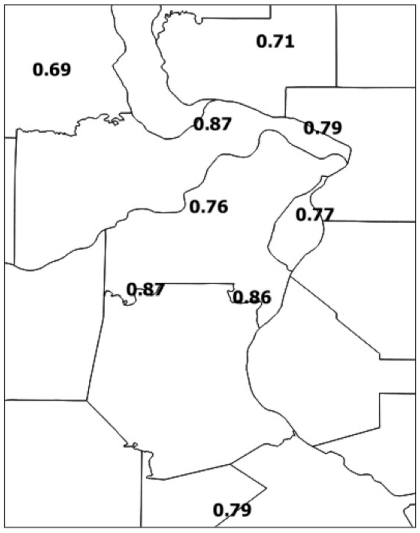

Figure 4. Correlation coefficients between model-calculated hourly values and observed surface concentrations at the nine operational monitoring sites in the St. Louis region, July 1-5, 2012. These coefficients were calculated using simulated and observed hourly concentrations during daylight hours: 1000 CDT to 1800 CDT. Lines indicate county boundaries within the greater St. Louis region.

Preprints (www.preprints.org) | NOT PEER-REVIEWED | Posted: 4 October 2017 doi:10.20944/preprints201708.0020.v3

Figure 5 depicts the distribution of ozone at the surface during the day (July 2) at four different times, as photochemical generation of ozone takes place. Low concentrations are visible in the morning (0600 LT), which are generally in the 35-40 ppb range near the city and surrounding environs. High concentrations are shown in the middle of the afternoon (1500 LT), with the highest approaching 90 ppb, consistent with the depiction of the St. Louis plume shown in the inset in Fig. 4b where "orange" AQI values denote a concentration of 71-85 ppb. These temporal and spatial patterns are also consistent with the general observation that the highest O_3 concentrations are found downwind of the urban area, and the surface plume identified in Figure 2b is well simulated by the model. Also depicted on these panels are three stars, which indicate representative locations upwind of the city, center of the city, and downwind of the city.

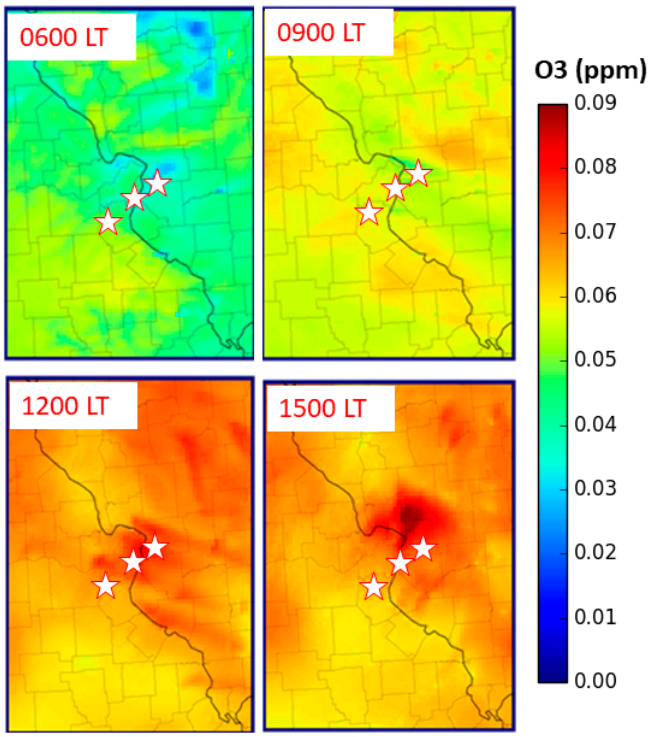

Figure 5. Evolution of the model-derived distribution of O_3 at the surface on July 2, 2012. The three stars show the locations of "upwind," "city," and "downwind" locations that will be discussed in more detail in the text and on subsequent figures.

Preprints (www.preprints.org) | NOT PEER-REVIEWED | Posted: 4 October 2017 doi:10.20944/preprints201708.0020.v3

Figure 6 compares model-derived diurnal surface concentrations at the starred locations shown in Figure 5. Over the city, highest concentrations are found early afternoon (1200-1400 LT), whereas at the downwind location, the highest concentrations are found later in the afternoon (after 1300), peaking in the early evening. Upwind concentrations do not peak as high as those found either over or downwind of the city during most hours. This is consistent with elevated O_3 seen at the surface, which is most likely most likely generated from the St. Louis's urban emissions.

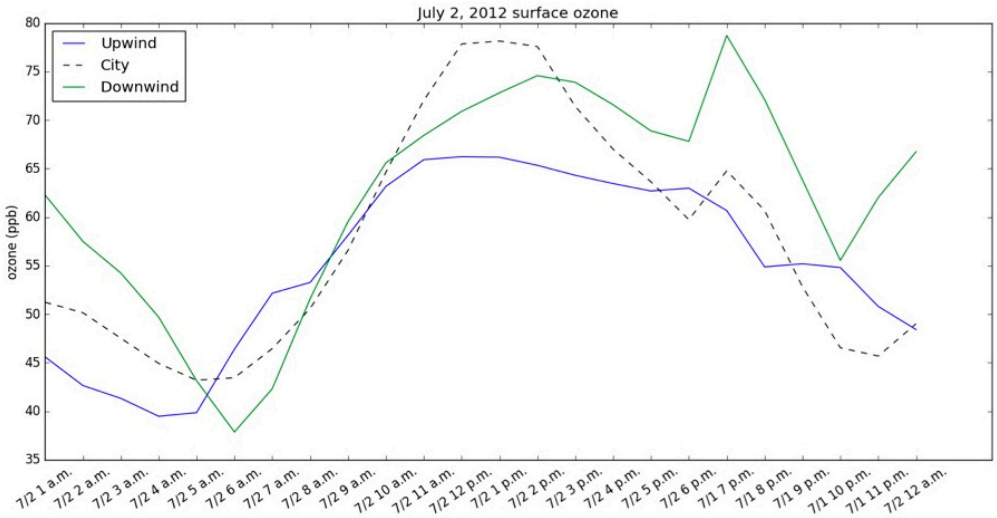

Figure 6. The model-derived diurnal concentrations of surface ozone at the upwind, city, and downwind locations shown in Figure 5.

Figure 7 shows model-derived ozone profiles in the lowest 10 km of the model at the three locations shown in Figure 5. Throughout the course of the day, ozone builds up in the lowest layers of the model, to ~3 km, and is transported with prevailing light southwesterly winds. As a result of this transport, we find highest integrated ozone amounts ozone downwind of the city, later in the day, relative to the integrated amount either over, or upwind of the city. Note that there is some variability in the ozone profiles above an altitude of 4 km, but since the air is less than half as dense in the middle and upper troposphere, the integrated amount of

Preprints (www.preprints.org) | NOT PEER-REVIEWED | Posted: 4 October 2017 doi:10.20944/preprints201708.0020.v3

ozone between 4 and 10 km contributes only a relatively small fraction compared to amount integrated below 4 km.

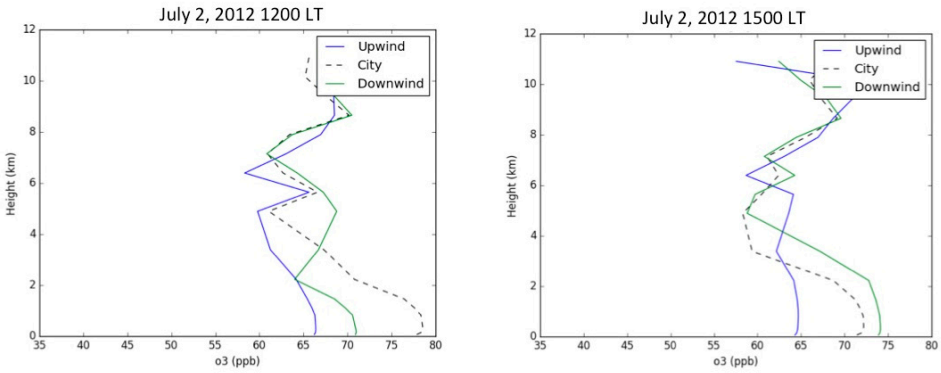

Figure 7. Model-derived profiles of O_3 concentration from the surface to 12 km for the three locations shown in Figure 5.

Of particular interest in this modeling study, are the depictions shown in Figure 8, which illustrates how the integrated amount of tropospheric ozone (0-10 km) varies regionally over the course of a day (i.e., July 2). Before the model photochemistry turns on with the rising sun, a very small gradient is found at 0600 LT. As the daytime photochemistry develops, a well-defined urban plume is found downwind of the city. This plume-like structure is more identifiable than what was calculated for the surface ozone concentrations shown in Figure 5. Within the plume, integrated values as high as 4.2 x 10^{17} mol. cm^{-2} are at 1500 LT. Integrated column amounts are more commonly measured in Dobson Units (DU), where 1 DU = 2.69 x 10^{16} molecules cm^{-2}. Thus, the plume emanating from St. Louis is ~16 DU, which is smaller than the TOMS/SBUV residual described in previous studies (Fishman et al. (1987; 2003). Explanations for these differences are discussed in the next section.

Preprints (www.preprints.org) | NOT PEER-REVIEWED | Posted: 4 October 2017 doi:10.20944/preprints201708.0020.v3

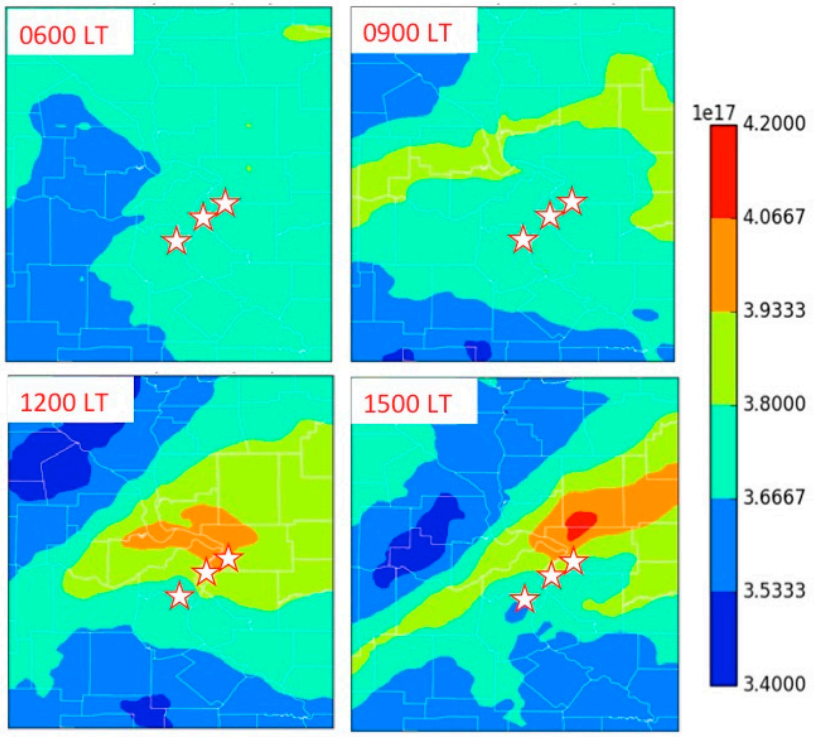

Figure 8. The column integrated amount of ozone generated by the model for four different times of the day on July 2, 2012.

IV Discussion

4a. Previous studies comparing satellite TOR with *in situ* measurements

Identification of enhanced total ozone column amounts were first published by Fishman et al. (1986) at tropical latitudes, where the enhancements were associated with widespread biomass burning in the Brazilian cerrado and subsequently, at middle latitudes (Fishman et al., 1987). The enhancements found within the TOMS elevated integrated amounts over Brazil were consistent with the *in situ* aircraft profiles measured in a 1980 NCAR field campaign (Crutzen et al., 1985). Subsequent measurements from the TRACE-A field campaign (Fishman et al., 1996a;b) included *in situ* aircraft and ozonesonde measurements, aircraft O_3 profiles from the UV-DIAL system, and satellite measurements, which confirmed that enhancements in the TOMS total ozone signal were a result of widespread biomass burning over Brazil and southern Africa. Because of low-level transport from the east out of southern Africa, where widespread burning was occurring and the upper-level transport from the west where ozone generated from burning over

Preprints (www.preprints.org) | NOT PEER-REVIEWED | Posted: 4 October 2017 doi:10.20944/preprints201708.0020.v3

Brazil had been carried to higher altitudes by convection and then transported in westerlies, highest TOR amounts were found over the south Atlantic Ocean, where these two plumes cross (Fishman et al., 1996a).

In terms of direct comparisons between TOR calculations and direct observations, we compared the satellite data with integrated tropospheric O_3 amounts obtained by the UV-DIAL system as the NASA DC-8 made several transit flights and found excellent agreement between the two datasets. Throughout the TRACE-A mission, there was relatively good agreement between the two methods that calculated integrated tropospheric ozone quantities except when heavy amounts of aerosols were present from the smoke emanating from vegetation burning (Fishman et al, 1996b).

When the east coast of the U.S. is dominated by a vast region of high pressure (when the "Bermuda High" is firmly established) resulting in conditions of widespread air stagnation (Korshover and Angell, 1982), numerous monitoring stations measure O_3 concentrations well above NAAQS standards. Analyses from Fishman at al. (1987) show that the persistent nature of such meteorological patterns could be defined as a synoptic scale event once AQS data were screened to remove the impact of urban-scale pollution generation. The top two panels in Figure 9 are taken from this study, and illustrate how this synoptic-scale ozone pollution episode can be identified within the distribution of total ozone measurements obtained from TOMS instrument aboard the Nimbus 7 satellite. The top panel depicts a vast area of the southeastern U.S., where daily maximum values exceeded 100 ppb at the surface. To be included in this analysis, all stations used in the analysis had been identified as not being directly downwind of an urban area. This large area of elevated ozone at the surface ozone grew over a 4-day period, as an intense anticyclone positioned itself over the eastern U.S. (Fishman and Balok, 1999).

Ground level ozone is the NAAQS pollutant most frequently in violation of the standard (NAS, 1991; https://www.uschamber.com/issue-brief/ozone-national-ambient-air-quality-standards#ozone_problems), but there have been only a couple of studies that relate TOR or TCO satellite-derived measurements to *in situ* O_3

Preprints (www.preprints.org) | NOT PEER-REVIEWED | Posted: 4 October 2017 doi:10.20944/preprints201708.0020.v3

concentrations. For validation, TOR and TCO have been compared with ozonesonde measurements (e.g., Fishman et al., 1990; Fishman and Balok, 1999; Ziemke et al., 2006), and have been shown to be in good agreement on both a climatological and seasonal basis. Fishman et al. (2010) compared monthly average surface O_3 over central Indiana with TOR over a 5-year period and found a statistically significant positive correlation. Fishman et al. (1990) compared monthly average 500-mb O_3 concentrations with TOR at several long-term ozonesonde sites and likewise found a strong positive correlation. Creilson et al. (2003) examined the seasonality of average TOR distributions with comparable integrated ozone amounts at five ozonesonde sites and noted excellent agreement with both the seasonality and the longitudinal gradient at northern middle latitudes.

During the 1980 pollution episode depicted in Fig. 9, UV-DIAL aircraft measurements from the PEPE/NEROS (Persistent Elevated Pollution Episode/Northeast Regional Oxidant Study) field campaign provided a vertical structure of ozone over the eastern U.S., which was then integrated to produce a tropospheric column quantity consistent with the horizontal gradient calculated in the TOR amounts. During the episode shown in Figure 9, continuous ozone profile measurements using the UV-DIAL system (Browell et al., 1985) made measurements on August 7, 1980 (the day before the depictions shown in Figure 9) in Pennsylvania and Ohio, as part of PEPE/NEROS. In terms of high ozone concentrations, this region was not as polluted as the pollution in the southeast on the following day (shown in the top panel), but concentrations as high as 110 ppb extended for a distance of more than 300 km to vertical depth of more than 1000 m. Concentrations of 90 ppb reached an altitude as high as 1.5 km along the flight path (Fishman et al., 1987). When integrated along the flight path, the integrated ozone column amounts ranged between 15 and 20 DU (4.0×10^{17} to 5.4×10^{17} mol. cm^{-2}). Because of the altitude limitation of the airplane during this time, and the fact that the UV-DIAL system was considerably less developed, measurements above this altitude likely would have found elevated O_3 concentrations resulting in integrated amounts in the troposphere being considerably greater.

Preprints (www.preprints.org) | NOT PEER-REVIEWED | Posted: 4 October 2017 doi:10.20944/preprints201708.0020.v3

436 The bottom panel is the distribution of satellite-derived tropospheric ozone
437 derived from the TOR technique described in Fishman et al. (2003), a modification
438 of the initial TOR dataset described in Fishman et al. (1990). The spatial resolution
439 of the satellite measurements (TOMS and SBUV) used to derive this distribution, is
440 approximately 100 km. Since these instruments were aboard the polar-orbiting
441 Nimbus-7 satellite, only one measurement per day is available. Despite this coarse
442 spatial resolution, the satellite measurements were able to capture a feature of
443 elevated surface ozone where the spatial extent of this specific episode was
444 approximately several hundred km.
445 A second massive air pollution episode (Figure 10) enveloped much of the
446 eastern U.S. occurred during the period July 2-13, 1988 (Fishman and Balok, 1999;
447 Fishman et al., 2003). This case study (Schlichtel and Husar, 1998, private
448 communication) was able to capture one of the most widespread ozone pollution
449 episodes ever observed, and stimulated studies of regional ozone pollution through
450 the Ozone Assessment Transport Group (OTAG; Parker and Blodgett, 1999). As
451 seen from the surface analysis, vast areas of the eastern U.S. exhibited surface
452 concentration >90 ppb and was later addressed in a reassessment of the surface
453 ozone issue (NAS, 1991). This study identified the inherent need to implement
454 nitrogen oxide emissions, where previously the emphasis on emission controls
455 focused on the reduction of the release volatile organic compounds.
456

Preprints (www.preprints.org) | NOT PEER-REVIEWED | Posted: 4 October 2017 doi:10.20944/preprints201708.0020.v3

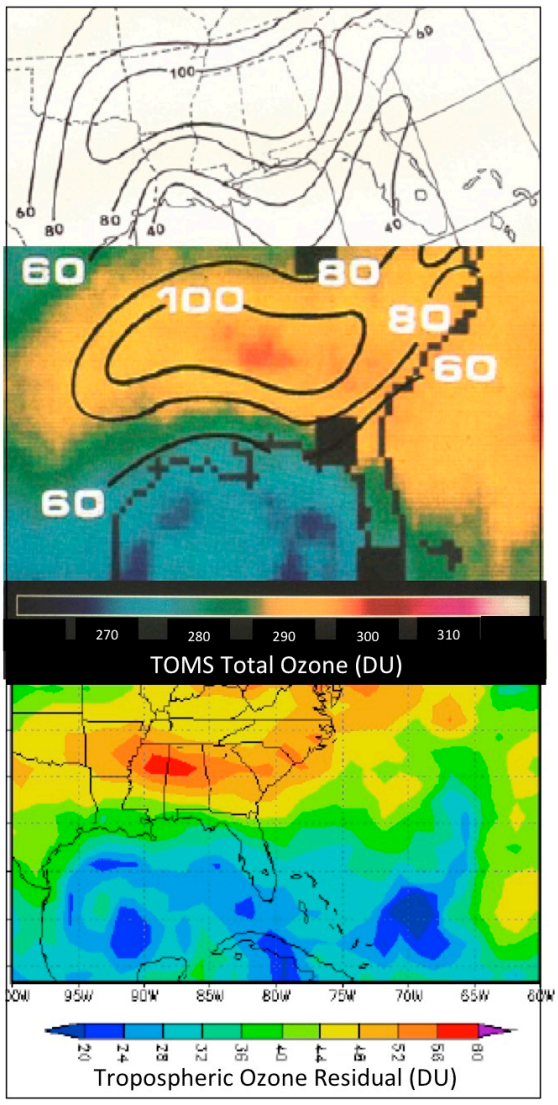

Figure 9. Historical perspective of observing ozone pollution episode from surface analysis and satellite measurements. The top two panels are from Fishman et al. (1987) showing the surface analysis of a synoptic-scale ozone pollution episode and the total ozone distribution from TOMS over the southeastern U.S. The surface analysis in the top panel is superimposed on the TOMS measurements in the middle panel. The bottom panel is from Fishman et al. (2003) and shows the calculated TOR distribution from TOMS and SBUV measurements for 8 August 1980. The unusually low TOR values coincide with the presence of Hurricane Allen, a Category 5 storm that was moving slowly in the Gulf of Mexico on this day before making landfall in east Texas on 11 August. We speculate that clean tropical air was feeding into the storm resulting in low tropospheric ozone concentrations being present as air spiraled into the storm's center.

Preprints (www.preprints.org) | NOT PEER-REVIEWED | Posted: 4 October 2017 doi:10.20944/preprints201708.0020.v3

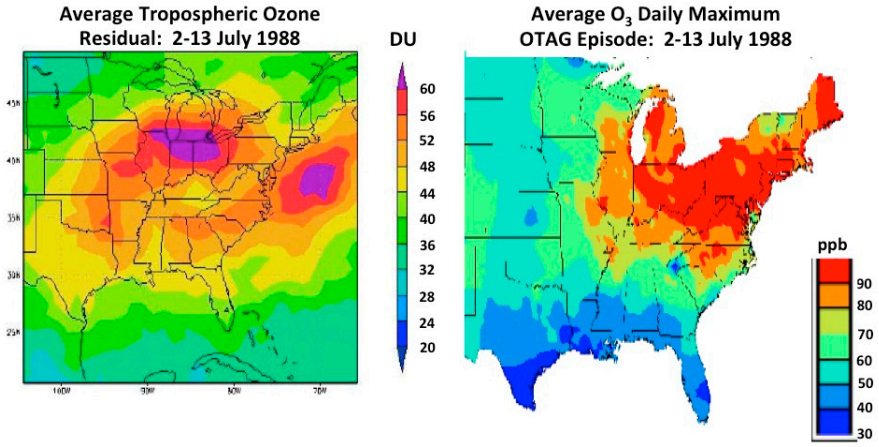

Figure 10 (left) Distribution of TOR during 2-13 July 1988 and the average daily ozone aximum for the same period (right). From Fishman et al. (2003) and Schlichtel and Husar (personal communication, 1998).

4b. Relevance of this modeling study to future satellite measurements

Within the next few years, TEMPO will be launched in geostationary orbit. In doing so, TEMPO, like OMI, GOME, and SCIAMACHY, will also derive its information via the application of a DOAS retrieval methodology to solar backscattered spectra in order to make measurements with hourly temporal resolution during the daytime. Furthermore, because TEMPO sits over one location and gathers information by "staring" for long periods of time over the entire United States (with parts of Mexico, Central America, and Canada also in its field of regard), it will be able to refine scales of only a few kilometers. However, despite the greatly enhanced spatial and temporal capability of TEMPO, no study has been conducted to relate these measurements to what might be present at the surface. The purpose of the set of results described in the previous section is to provide an analysis of a regional photochemical-transport model simulation to study the relationship between the integrated quantities that will be measured by TEMPO to the surface concentrations calculated at the surface for both ozone and NO_2.

Preprints (www.preprints.org) | NOT PEER-REVIEWED | Posted: 4 October 2017 doi:10.20944/preprints201708.0020.v3

4c. Model results post-2005 NO_2 emission standards

Because of the success of the implementation of emission controls, detection of regional-scale outbreaks of an ozone episode may prove more challenging now than when the NAAQS standards were first developed in the 1970s. We have analyzed all the available St. Louis AQS ozone measurements dating back to 1980 and calculated number of 8-hour daily maximum through 2016. When ozone standards were first established, they were based on concentrations over a 1-hr period then redefined in 1999 using an 8-hr standard after physiological research revealed longer exposure to high ozone at elevated concentrations was more damaging to human health than a relatively shorter exposure time after of 1 hour, even at higher concentrations (125 ppb), which was the original NAAQS standard. Over the years, approximately 10 monitors have operated in the greater St. Louis region, including both Missouri and Illinois. When analyzed in this manner, the years 1983 and 1988 produced more than 200 exceedances. In 1980, our analysis yielded more than 150 exceedances, but only five monitoring stations were operating in the first year of the St. Louis network. On a national level, EPA (2004) finds 1980, 1983 and 1988 as the years of highest concentration prior to the implementation of stricter NO_2 emission controls.

Over the last decade of observations, the summer of 2012 was the most polluted year in St. Louis with exceedances reaching 75. There is a strong correlation between summertime temperatures and ozone; 2012 was the hottest year on record in St. Louis since since routine pollution monitoring began. Thus, despite the record heat, U.S. regional emission controls (especially those for NO_2 implemented in 2005) suggest that ozone pollution has been greatly reduced (see Duncan et al., 2016).

4d. Calculation of surface and integrated nitrogen dioxide

The atmospheric residence time of NO_2 nitrogen dioxide is very short relative to other pollutants and goes through rapid conversion to nitric (NO) through photolysis. However, because of the ubiquitous presence of ozone throughout the troposphere, the NO generated from NO_2 photolysis reacts rapidly with O_3 to put

Preprints (www.preprints.org) | NOT PEER-REVIEWED | Posted: 4 October 2017 doi:10.20944/preprints201708.0020.v3

554 NO_2 back into the system. These rapid interconversion reactions between NO, NO_2
555 and O_3 are often referred to as the photostationary steady state (Calvert, 1976).
556 Figure 11a shows the calculated surface NO_2 concentrations at the three locations
557 identified in Figure 5. Many of these concentrations are below the detection limit of
558 routinely operating instruments, which have a detection lower limit of 1 ppb.
559 The integrated amount of NO_2 over the period of the model run is shown in
560 Figure 11b for each of the three locations in Figure 5. The highest NO_2 integrals are
561 generally found over the city center. There are a few instances when the values
562 downwind on a specific day exceed the amount over the city. The day-to-day
563 variability is dependent on a number of factors, including photochemistry,
564 transport, and the daily pattern of the NO_x (primarily NO) emissions that increase
565 considerably due to the varying nature of vehicular emissions, which correlate
566 highly with rush-hour traffic. The concentrations at the upwind location are always
567 lower than what is calculated over the city or downwind of it, suggesting that the St.
568 Louis metropolitan area is the primary reason for the generation of surface O_3 and
569 the O_3 formation downwind.
570 Background (i.e., upwind) integrated NO_2 amounts are calculated to be ~0.25
571 x 10^{15} mol. cm^{-2}, whereas urban values are generally 5-10 times larger and can
572 approach 2.5 x 10^{15} mol. cm^{-2}. Such amounts are well above the threshold level for
573 detection of NO_2 column amounts, but are somewhat near the low end of values
574 measured over other urban areas (Cede et al., 2006), which is not surprising since
575 most of those measurement were obtained before the implementation of the 2005
576 emission controls.
577 Using a reasonable simulation of a 5-day time period for O_3, when elevated
578 surface ozone concentrations above the NAAQS standard were present, the model
579 calculations in this study show the integrated column amounts of ozone to be
580 enhanced by as much as 20%. On the other hand, the model calculates a
581 considerably larger spatial variability for NO_2 column amounts; urban values are as
582 much as ten times the amount calculated for locations upwind of the city.
583
584

Preprints (www.preprints.org) | NOT PEER-REVIEWED | Posted: 4 October 2017 doi:10.20944/preprints201708.0020.v3

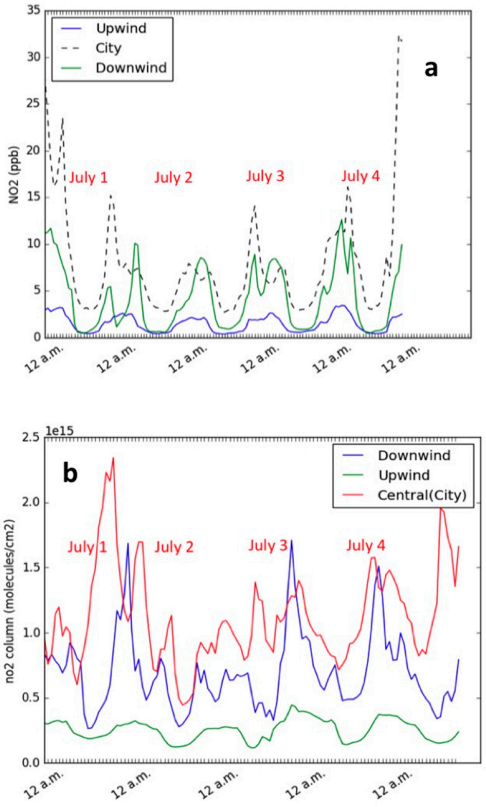

Figure 11(a) Model-derived surface NO_2 concentrations for the period July 1-5, 2012. The three curves show the values at the three locations shown in Figure 6. (b) Model-derived integrated NO_2 concentrations for the period July 1-5, 2012. The three curves show the values at the three locations shown in Figure 5.

These calculations are consistent with the early findings of Noxon (1979), who measured tropospheric column amount as low as 3 x 10^{14} mol. cm^{-2} in the mountains of Colorado, and more than 5 x 10^{15} mol. cm^{-2} when the Denver plume passed over his ground-based spectrometer. Our model-derived calculations show that total column amounts over and downwind of the St. Louis metropolitan area are generally close to 2 x 10^{15} mol. cm^{-2}, which are approximately five times larger than the amount calculated upwind. These regional tropospheric enhancements are readily identifiable and have been reported in the literature on numerous occasions (e.g., Lamsal et al., 2008; 2014).

Preprints (www.preprints.org) | NOT PEER-REVIEWED | Posted: 4 October 2017 doi:10.20944/preprints201708.0020.v3

V. Summary

This model study focused on analyzing the three-dimensional structure of ozone generated during a pollution event in St. Louis in 2012. We calculated a regional enhancement of ~30 ppb, in which many exceedances of the NAAQS O_3 standard occurred. Concentrations maximize at ~90 ppb whereas the background daytime concentrations measure approximately 60 ppb; these concentrations are consistent with the analyses shown in Fishman et al. (2010; 2014), which showed that summer summertime daytime O_3 concentrations average between 48 and 60 ppb at latitudes representative of St. Louis. These ozone-plume enhancements are consistent with data at the monitoring network in the St. Louis and correlation coefficients between the observed and model concentrations range from 0.69 to 0.87 at each of the nine monitoring sites. The integrated amount of O_3 in this pollution plume is calculated to be ~16 DU and primarily confined to the lowest 3 km of the model's vertical domain. Compared to areas within the computational domain outside the plume, this enhancement corresponds to an increase of ~0.6 x 10^{17} mol. cm^{-2}, or ~2-3 DU.

As a background to this study, we showed that widespread synoptic-scale pollution episodes covered the eastern U.S. in the 1980s, and identified two specific synoptic-scale episodes (hundreds of km) episodes in 1980 and 1988. Examination of aircraft measurements from the UV-DIAL system aboard a NASA research aircraft taking measurements in the PEPE/NEROS field study found enhanced ozone concentrations >110 ppb over a domain that stretched ~300 km up to an altitude higher than 1 km (Fishman et al., 1987). Such an episode generates an enriched air mass of ozone that is as high as 60 DU, which is more than 20 DU above the background integrated ozone amounts. Furthermore this episode is observed on a scale of more than several hundred km. However, through the implementation of emission controls over the past several decades, the presence of air pollution episodes on this large of a spatial scale have been virtually eliminated. In this particular study of St. Louis, the plume of elevated ozone extends marginally more than 200 km before it runs off the computational domain and is considerably smaller in scale that those identified in 1980 and 1988.

Preprints (www.preprints.org) | NOT PEER-REVIEWED | Posted: 4 October 2017 doi:10.20944/preprints201708.0020.v3

Returning to the AQI depiction shown for July 2, 2012, in Figure 2b, virtually no "red" areas (O_3 > 85 ppb) are found in the eastern U.S. A qualitative analysis of the Airnow archive (dating back to 2012) does not show the presence of vast areas of "unhealthy" air, where O_3 > 86 ppb. On the contrary, Figures 9 and 10, show wide areas where concentrations of more than 90 ppb are present. Although it is difficult to provide a definitive quantitative estimate comparing pollution episodes identified in 1980 and 1988 with the modeling study presented here, it is clear that the magnitude and spatial extent of the situation modeled in this study are considerably less than what was observed then. The conclusion we draw from our model calculations and the qualitative analysis of ozone pollution episodes from 2012 onwards is that there has been a significant reduction in ozone pollution in the past decade compared with the 1980s. Despite this being a positive accomplishment for air quality managers, it points to capability hurdles in observing present-day and future ozone pollution events once TEMPO is launched, presenting a greater challenge now than if the satellite had been launched in the 1980s.

For NO_2, the model calculations show that concentrations are highest over the city, consistent with other analyses of satellite measurements (e.g., Noxon, 1978; Cede et al., 2006; Duncan et al., 2016). The integrated gradients calculated by the model show spatial gradients where values generally differ by a factor of 4 to 5, consistent with other observations from satellites and thus should be readily observable from space. Lastly, Fishman et al. (2014) identified the paradoxical analysis that ozone generated from pollution episodes is decreasing in St. Louis, while background concentrations are increasing. This phenomenon is likely due to long-range transport from across the Pacific (Cooper et al., 2017). Such a finding similarly suggests that episodes resulting in a violation of the NAAQS O_3 standard are likely smaller in magnitude when contrasted against background O_3 concentrations, and therefore more challenging to identify from future TEMPO measurements. Lastly, observing NO_2 in the troposphere from space is considerably less challenging over urban areas since the contribution from urban areas is several times larger than the contribution from NO_2 in the stratosphere. Alternatively, observing the O_3 enhancement simulated here is considerably more challenging

Preprints (www.preprints.org) | NOT PEER-REVIEWED | Posted: 4 October 2017 doi:10.20944/preprints201708.0020.v3

since the overlying ozone burden of O_3 in the stratosphere is generally ten times greater than the integrated amount generated during an air pollution episode.

Acknowledgements

We thank Dr. Alex Cohan of LADCO (Lake Michigan Air Directors Consortium) for working with us to get the CAMx model to run for this study. Financial support for this research came from NASA's AQAST (Air Quality Applications Science Team) under NASA grant NNX11AJ6 and from the TEMPO Project Office located at the Smithsonian/Harvard Astrophysical Observatory under subcontract SV3-83017 to Saint Louis University . The authors also thank Ms Carolyn Fernandez of the Department of Earth & Atmospheric Sciences for her technical assistance in the preparation of this manuscript.v

Preprints (www.preprints.org) | NOT PEER-REVIEWED | Posted: 4 October 2017 doi:10.20944/preprints201708.0020.v3

691 References

692

693 Browell, E.V.; Carter, A.F.; Shipley, S.T.; Allen, R.J.; Butler, C.F.; Mayo M.N.; Siviter,
694 J.H.; and Hall, W.M., NASA multipurpose airborne DIAL system and measurements of
695 ozone and aerosol profiles, *Appl. Opt,,* **1985,** *22*, 522-534.

696 Brasseur G.; and Solomon, S., *Aeronomy of the Middle Atmosphere (2nd ed.)*, Reidel,
697 Dordrecht, Holland, 1986, pp. 144-157.
698
699 Calvert, J.G. Test of the theory of ozone generation in Los Angeles atmosphere. *Env. Sci.*
700 *Tech.*, **1976**. ***10***, 248-262.
701
702 Cede, A.; Herman, J.; Richter, A.; Krotkov, N.; Burrows, J. Measurements of nitrogen
703 dioxide total column amounts using a Brewer double spectrophotometer in direct Sun
704 mode, *J. Geophys. Res.,* **2006**, *111*, D05304, doi:10.1029/2005JD006585.
705
706 Cooper, O.R., et al. (17 authors), Global distribution and trends of tropospheric ozone:
707 An observation-based review, *Elementa*, **2017**, *2*, doi:
708 10.12952/journal.elementa.000029.elementascience.org
709
710 Creilson, J.K., Fishman, J., Wozniak, A.E., Intercontinental transport of tropospheric
711 ozone: A study of its seasonal variability across the North Atlantic utilizing tropospheric
712 ozone residuals and its relationship to the North Atlantic Oscillation, *Atmos. Chem.*
713 *Phys.*, **2003**, *3*, 2053-2066 (http://www.atmos-chem-phys.org/acp/3/2053)
714
715 Crutzen, P. J.;. Delany, A.C.; Greenberg, J.;Haagenson, P.; Heidt, L.; Lueb, R.; Pollock,
716 W.; Seiler, W.; Wartburg A.; Zimmerman, P. Tropospheric chemical composition
717 measurements in Brazil during the dry season, . *Atmos. Chem*., **1985**, *2*, 233-256.
718
719 De Foy, B., , Lu, A., Streets, D.G., Impacts of control strategies, the Great Recession and
720 weekday variations on NO2 columns above North American cities, *Atmos. Env.,***2016**,
721 138, 74-86 (http://dx.doi.org/10.1016/j.atmosenv.2016.04.038)
722
723 Duncan, B.N., et al. (25 authors). Satellite Data of Atmospheric Pollution for U.S. Air
724 Quality Applications: Examples of Applications, Summary of Data End-User Resources,
725 Answers to FAQs, and Common Mistakes to Avoid, *Atmos. Environ.,* **2016**,
726 doi:10.1016/j.atmosenv.2014.05.061.
727
728 EPA, The Ozone Report: Measuring Progress through 2003, U.S. EPA 454/K-04-001,
729 April 2004, Research Triangle Park NC, 23pp. (Available on line at:
730 https://nepis.epa.gov/Exe/ZyNET.exe/10004DTX.txt?ZyActionD=ZyDocument&Clie
731 nt=EPA&Index=2000%20Thru%202005&Docs=&Query=&Time=&EndTime=&Sear
732 chMethod=1&TocRestrict=n&Toc=&TocEntry=&QField=&QFieldYear=&QFieldMont
733 h=&QFieldDay=&UseQField=&IntQFieldOp=0&ExtQFieldOp=0&XmlQuery=&File=D
734 %3A%5CZYFILES%5CINDEX%20DATA%5C00THRU05%5CTXT%5C00000008%5C
735 10004DTX.txt&User=ANONYMOUS&Password=anonymous&SortMethod=h%7C-

Preprints (www.preprints.org) | NOT PEER-REVIEWED | Posted: 4 October 2017 doi:10.20944/preprints201708.0020.v3

&MaximumDocuments=1&FuzzyDegree=0&ImageQuality=r75g8/r75g8/x150y150g16/i425&Display=hpfr&DefSeekPage=x&SearchBack=ZyActionL&Back=ZyActionS&BackDesc=Results%20page&MaximumPages=1&ZyEntry=2)

Fishman, J.; Balok, A.E. Calculation of Daily Tropospheric Ozone Residuals Using TOMS and Empirically-Improved SBUV Measurements: Application to an Ozone Pollution Episode over the Eastern United States, *J. Geophys. Res.,* **1999**, *104*, 30,319-30,340.

Fishman, J.; Minnis, P.; Reichle, Jr., H. G.: The Use of Satellite Data to Study Trace Gas Emissions in the Tropics. *J. Geophys. Res*., **1986**, *91*, No. D13, 14451-14465.

Fishman, J.; Vukovich, F. M.; Cahoon, D. R.; and Shipham, M. C. The Characterization of an Air Pollution Episode Using Satellite Total Ozone Measurements. *J. Clim. Appl. Meteor*. **1987**, *26*, 1623-1654.

Fishman, J.; Hoell, Jr., J.M.; Bendura, R.D.; Kirchhoff, V.W.J.H.; McNeal, R.J. The NASA GTE TRACE-A Experiment (September-October, 1992), *J. Geophys. Res.,* **1996a** *101*, D19, 23,865-23,879.

Fishman, J.; Brackett, V.G.; Browell, E.V.; Grant, W.B. Tropospheric Ozone Derived from TOMS/SBUV Measurements during TRACE-A, *J. Geophys. Res.* **1996b,** *101,* 24,069-24,082.

Fishman, J.; Wozniak, A.E.; Creilson, J.K. Global distribution of tropospheric ozone from satellite measurements using the empirically corrected tropospheric ozone residual technique: Identification of the regional aspects of air pollution, *Atmos. Chem. Phys.,* **2003,** *3,* 893-907, (www.atmos-chem-phys.org/acp/3/893/).

Fishman, J.; Creilson, J.K.; Parker, P.A.; Ainsworth, E.A.; Vining, G.G.; Szarka, J.; Booker, F.L.; Xu, X. An investigation of widespread ozone damage to the soybean crop in the upper Midwest determined from ground-based and satellite measurements, *Atmos. Environ.* **2010,** doi:10.1016/jatmosenv.2010.01.015.

Fishman, J.; Belina, K.M.; Encarnaciòn, C.H The St. Louis Ozone Gardens: Visualizing the impact of a changing atmosphere, *Bull. Amer. Meteor. Soc.,* **2014**, *85,*1171-1176.

Korshover, J., Angell, J.K., A review of air stagnation cases in the eastern United States in 1981—Annual summary, *Mon. Wea. Rev.* **1982**, *110*, 1515-1518.

Lamsal, L.N., Martin, R.V., Steinbacher, M., Celarier, E. A., Bucsela, E., Dunlea, E. J., and Pinto, J.: Ground level nitrogen dioxide concentrations inferred from the satellite-borne Ozone Monitoring Instrument, *J. Geophys. Res.,* **2008,***113*, 35 doi:10:1029/2007DJ009235.

Preprints (www.preprints.org) | NOT PEER-REVIEWED | Posted: 4 October 2017 doi:10.20944/preprints201708.0020.v3

781 Lamsal, L. N., Krotkov, N. A., Celarier, E. A., Swartz, W. H., Pickering, K. E., Bucsela,
782 E. J., Gleason, J. F., Martin, R. V., Philip, S., Irie, H., Cede, A., Herman, J., Weinheimer,
783 A., Szykman, J. J., and Knepp, T. N.: Evaluation of OMI operational standard NO2
784 column retrievals using in situ and surface-based NO2 observations, *Atmos. Chem. Phys.,*
785 **2014,** *14*, 11587–11609,
786

787 Lamsal, L.N., Duncan, B.N., Yoshida, Y., Krotkov, N.A., Pickering, K.E., Streets, D.G., Lu,
788 Z., U.S. NO2 trends (2005-2013): EPA Air Quality System (AQS) data versus
789 improved observations from the Ozone Monitoring Instrument (OMI), , *Atmos.*
790 *Env.,***2015**, 130, 74-86, (hhttp://dx.doi.org/10.1016/j.atmosenv.2015.03.055)
791

792 Levelt, P. et al. (44 co-authors) The Ozone Monitoring Instrument: Overview of
793 twelve years in space, *Atmos. Chem. Phys. Disc.* **2017** *(*https://doi.org/10.5194/acp-
794 2017-487)
795

796 Lu, Z.; Streets, D. G.; de Foy, B.; Lamsal, L. N.; Duncan, B.N.; Xing, X. Emissions of
797 nitrogen oxides from US urban areas: estimation from Ozone Monitoring Instrument
798 retrievals for 2005-2014, *Atmos. Chem. Phys.,* **2015,***15*, 10367-10383,
799

800 NAS, *Rethinking the Ozone Problem in Urban and Regional Air Pollution*, National
801 Academies Press, Washington DC, **1991**,524 pp. (pdf available at
802 http://www.nap.edu/catalog/1889.html.)
803

804 Parker, L., J. Blodgett, J. *Air Quality: EPA's Ozone Transport Rule, OTAG, and Section*
805 *126 Petitions -- A Hazy Situation*? **1999**, (available from National Digital Library,
806 retrieved July 2017)
807 (https://digital.library.unt.edu/ark:/67531/metacrs935/m1/1/high_res_d/98-
808 236_1999Jun15.html#Back4)
809

810 Platt, U., Stutz, J. **2008**. *Differential Optical Absorption Spectroscopy*. *Springer*, Berlin,
811 Germany, 597 pp.
812

813 Russell, A.R.; Valin, L. C.; Cohen, R.C. Trends in OMI NO2 observations over the
814 United States: effects of emission control technology and the economic recession,
815 *Atmos. Chem. Phys.,* **2012**, *12*, 12197–12209, ,www.atmos-chem-
816 phys.net/12/12197/2012/ doi:10.5194/acp-12-12197-2012

817 Ziemke, J. R.; Chandra, S.; and Bhartia, P. K.: Two new methods for deriving
818 tropospheric column ozone from TOMS 35 measurements: The assimilated UARS
819 MLS/HALOE and convective-cloud differential techniques, *J. Geophys. Res., 103*, **1998**,
820 doi:10.1029/98JD01567, 22,115-22,127,.

821 Ziemke, J. R.; Chandra, S.; Duncan, B. N.; Froidevaux, L.; Bhartia, P. K.; Levelt, P. F.;
822 Waters, J. W. Tropospheric ozone determined from Aura OMI and MLS: Evaluation of

Preprints (www.preprints.org) | NOT PEER-REVIEWED | Posted: 4 October 2017 doi:10.20944/preprints201708.0020.v3

823 measurements and comparison with the Global Modeling Initiative's Chemical Transport
824 Model, *J. Geophys. Res.,* **2006**, *111*, D19303, doi:10.1029/2006JD007089,.

825
826 Ziemke, J. R.; Olsen, M. A.; Witte, J. C.; Douglass, A. R.; Strahan, S. E.; Wargan, K.;
827 Liu, X.; Schoeberl, M. R.; Yang, K.; Kaplan, T. B,; Pawson, S.; Duncan, B. N.; Newman,
828 P. A.; Bhartia, P. K.; Heney, M. K. Assessment and applications of NASA ozone data
829 products derived from Aura OMI/MLS satellite measurements in context of the GMI
830 Chemical Transport Model, *J. Geophys. Res.,* **2014**, *119,* 5671-5699,
831 doi:10.1002/2013JD020914,.
832

833 Zoogman, P., et al. (39 co-authors), Tropospheric Emissions: Monitoring of Pollution
834 (TEMPO), *J. Quant. Spectroscopy Rad. Transfer,* **2017**, ***186***, (in press)
835 (http://dx.doi.org/10.1016/j.jqsrt.2016.05.008)
836